JACS
JOURNAL OF THE AMERICAN CHEMICAL SOCIETY
pubs.acs.org/JACS
Communication

Triple Resonance Experiments for the Rapid Detection of ^{103}Rh NMR Shifts: A Combined Experimental and Theoretical Study into Dirhodium and Bismuth−Rhodium Paddlewheel Complexes

Fabio P. Caló, Giovanni Bistoni, Alexander A. Auer, Markus Leutzsch,* and Alois Fürstner*

Cite This: J. Am. Chem. Soc. 2021, 143, 12473−12479
Read Online
ACCESS | Metrics & More | Article Recommendations | Supporting Information

ABSTRACT: A H(C)Rh triple resonance NMR experiment makes the rapid detection of ^{103}Rh chemical shifts possible, which were previously beyond reach. It served to analyze a series of dirhodium and bismuth−rhodium paddlewheel complexes of the utmost importance for metal−carbene chemistry. The excellent match between the experimental and computed ^{103}Rh shifts in combination with a detailed analysis of the pertinent shielding tensors forms a sound basis for a qualitative and quantitative interpretation of these otherwise (basically) inaccessible data. The observed trends clearly reflect the influence exerted by the equatorial ligands (carboxylate versus carboxamidate), the axial ligands (solvents), and the internal "metalloligand" (Rh versus Bi) on the electronic estate of the reactive Rh(II) center.

For a shift range on the order of 12.000 ppm, ^{103}Rh NMR spectroscopy is, a priori, a cardinal tool to probe the electronic nature of a given rhodium complex. It allows even small electronic and geometric changes in the coordination sphere to be detected, which are difficult, if not even impossible, to assess otherwise.[1−4] Its exceptional responsiveness to the chemical environment notwithstanding, ^{103}Rh NMR is not nearly as routinely used by practitioners as one might assume. An extremely low gyromagnetic ratio in combination with often unduly long relaxation times[5] offsets the inherent advantages of ^{103}Rh as an $I = 1/2$ nucleus of 100% natural abundance.[6−8] 2D inverse detection techniques based on polarization transfer, most notably HMQC experiments, are the currently best way to overcome this massive hurdle (Scheme 1); they mandate, however, that a sensitive nucleus (^{1}H or ^{31}P) is (directly) coupled to the Rh-center, which in turn limits the types of complexes that can be covered.[1−4]

Scheme 1. Established and New Methods for the Determination of ^{103}Rh Chemical Shifts

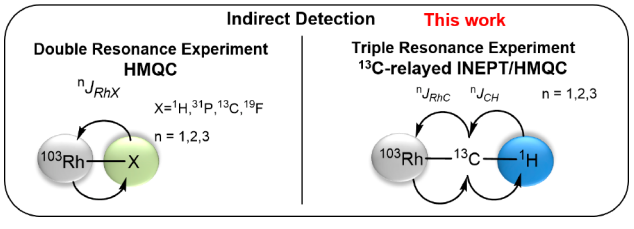

Because dirhodium tetracarboxylate complexes lack these requirements, such "paddlewheel" compounds have basically defied scrutiny by ^{103}Rh NMR spectroscopy despite their paramount importance in (asymmetric) carbene chemistry and beyond.[9−21] Not even the ^{103}Rh chemical shifts of bare unquenched $[Rh_2(OAc)_4]$ (**1**) or $[Rh_2(OTfa)_4]$ (**6**) are known,[22−27] which are the parent members of this series and the starting points for the preparation of innumerous chiral variants by ligand exchange. Outlined below is a convenient NMR experiment that applies to these and other rhodium complexes that were previously beyond reach. A combined experimental and computational approach helps to interpret the now available shift data and in so doing provides insights into the electronic nature of these valuable catalysts.[28−30]

The key to success was the adaptation of a proton-detected triple resonance experiment to the current problem, which draws its high sensitivity from the initial excitation and the final detection of ^{1}H (Scheme 1).[31] After extensive testing, a pulse sequence introduced by Mobley and co-workers was found to give the best results (Figure 1).[32−35] In the essence, intensive nuclei enhancement by polarization transfer (INEPT) is used for a first magnetization transfer from ^{1}H to ^{13}C as the relay atom, followed by a heteronuclear multiple quantum correlation (HMQC) transfer from ^{13}C to ^{103}Rh.[36]

$[Rh(acac)_3]$ was chosen for the initial tests because the early literature explicitly stated that the ^{103}Rh shift of this compound can only be determined by direct observation.[7] The triple resonance experiment clearly proves this wrong; it was optimized for magnetization transfer from the protons to the C═O signal (δ_C = 188.8 ppm, $J_{C,H}$ = 4 Hz) and from ^{13}C to ^{103}Rh ($J_{C,Rh}$ = 1.1 Hz).[38] The spectrum shown in Figure 2 was recorded in 4 min with a 10 mM solution in $CDCl_3$ using nonuniform sampling in the indirect dimension; this result is

Received: June 21, 2021
Published: August 5, 2021

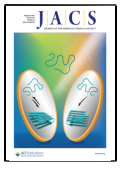

ACS Publications
© 2021 The Authors. Published by American Chemical Society

https://doi.org/10.1021/jacs.1c06414
J. Am. Chem. Soc. 2021, 143, 12473−12479

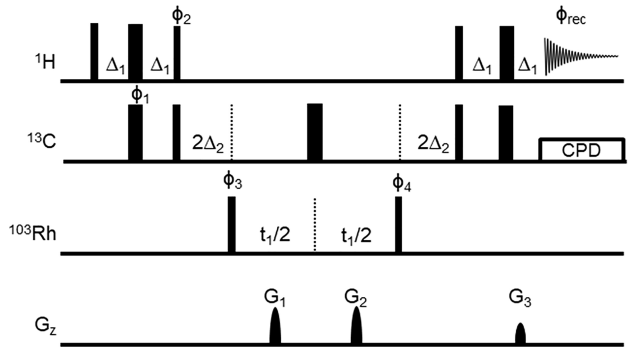

Figure 1. H(C)Rh pulse sequence. The phase cycling scheme is as follows: x = pulses without a defined phase; Φ_1 = $x, x, x, x, -x, -x, -x, -x$; Φ_2 = y; Φ_3 = $x, -x$; Φ_4 = $x, x, -x, -x$; Φ_{rec} = $x, -x, -x, x$. Gradient ratios are as follows: for concentrated samples, G_1 = 75%, G_2 = 32%, and G3 = 14.2%; for diluted samples, G_1 = G_2 = 80%, G_3 = 5.1%, g_{max} = 51.3 G/cm, $\Delta_1 = 1/(4 \times J_{CRh})$; $\Delta_2 = 1/(4 \times J_{CRh})$ for monomeric Rh complexes, $\Delta_2 = 1/(12 \times J_{CRh})$ for dinuclear Rh(II) paddlewheel complexes.

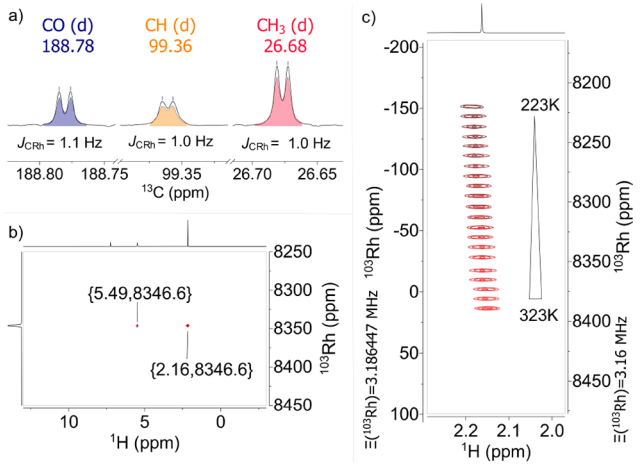

Figure 2. (a) $^{13}C\{^1H\}$ NMR signals of $Rh(acac)_3$. (b) H(C)Rh spectrum of $Rh(acac)_3$ (10 mM). (c) ^{103}Rh chemical shift of $Rh(acac)_3$ at temperatures between 223 and 323 K; the left axis shows the ^{103}Rh chemical shift referenced according to IUPAC recommendations (saturated $Rh(acac)_3$ in $CDCl_3$ (δ = 0 ppm), $\Xi(^{103}Rh)$ = 3.186447%), and the right axis uses the commonly applied reference ($\Xi(^{103}Rh)$ = 3.16%)).[37]

deemed remarkable in view of a T_1-relaxation time of 39 s (at 9.4 T and 310 K).[5] The known temperature-dependence of the resonance (1.6 ppm/K) could be easily verified.[1,37]

The situation in $[Rh_2(OAc)_4]$ is slightly more involved because the magnetization will be transferred from one C atom to two chemically equivalent Rh centers. In contrast to a mononuclear complex where the magnetization transfer efficiency of the HMQC step is $\Delta_2 = 1/(4 \times J_{CRh})$, the optimal delay for an IS_2 system is theoretically $\Delta_2 = 1/(8 \times J_{CRh})$.[39] In our case, however, best results were obtained with $\Delta_2 = 1/(12 \times J_{CRh})$ (see the Supporting Information). Under these conditions, excellent spectra were recorded with 10−15 mM solutions of isotopically *unlabeled* $[Rh_2(OAc)_4]$ in $[D_3]$-MeCN with a ≤15 min acquisition time regardless of whether the magnetization transfer pathway I or II was chosen (Figure 3).[40] Once again, the strong temperature-dependence of the signal (1.33 ppm/K) was easily proven.[41]

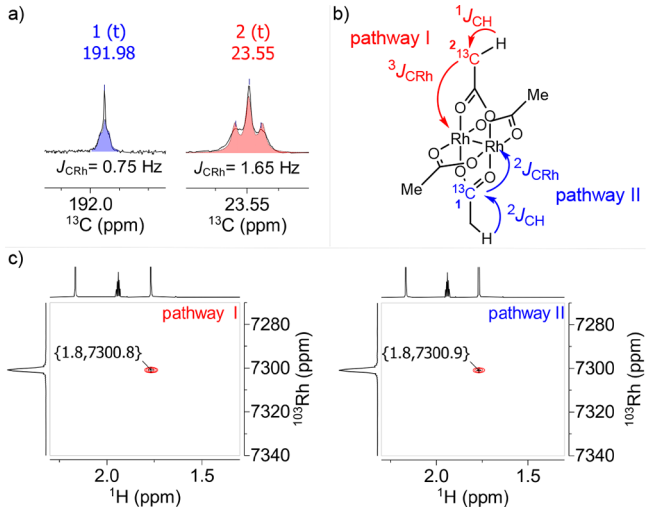

Figure 3. (a) $^{13}C\{^1H\}$ NMR signals of $[Rh_2(OAc)_4]$ (**1**) in CD_3CN. (b) Magnetization transfer pathways. (c) H(C)Rh spectra (15 mM) using pathway I or II.

Because acetonitrile acts as kinetically labile ligand to the axial coordination sites on the dimetallic cage of **1**, the effect of different solvents was evaluated (Scheme 2A). The recorded

Scheme 2. Two Different Test Sets Showing the Influence of the (A) Axial and (B) Equatorial Ligands

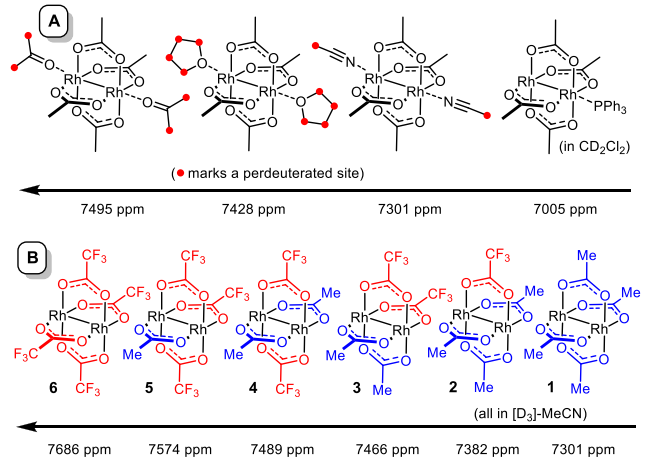

data suggest that $[D_8]$-THF and $[D_6]$-acetone as supposedly weaker donors than MeCN cause a "deshielding" of the signal, whereas the analogous (catalytically inactive) adduct **1**·PPh_3 has a notably lower shift.[42−44]

Next, the influence of the bridging carboxylate ligands was studied more systematically. To this end, all possible (heteroleptic) dirhodium acetate and trifluoroacetate complexes (**1**−**6**) were prepared and analyzed (Scheme 2B).[45,46] The recorded data provide a dramatic illustration of the sensitivity of ^{103}Rh chemical shifts to changes in the periphery of the nucleus; remote fluorination entails incremental deshielding over a range of no less than 380 ppm. Qualitatively, increased electrophilicity at the rhodium seems to come along with higher δ_{Rh}; to scrutinize this aspect, this particular set of complexes was chosen for a detailed computational analysis (see below).

Numerous other dirhodium tetracarboxylate complexes could be analyzed equally well (Figure 4). The recorded δ_{Rh}

https://doi.org/10.1021/jacs.1c06414
J. Am. Chem. Soc. 2021, 143, 12473−12479

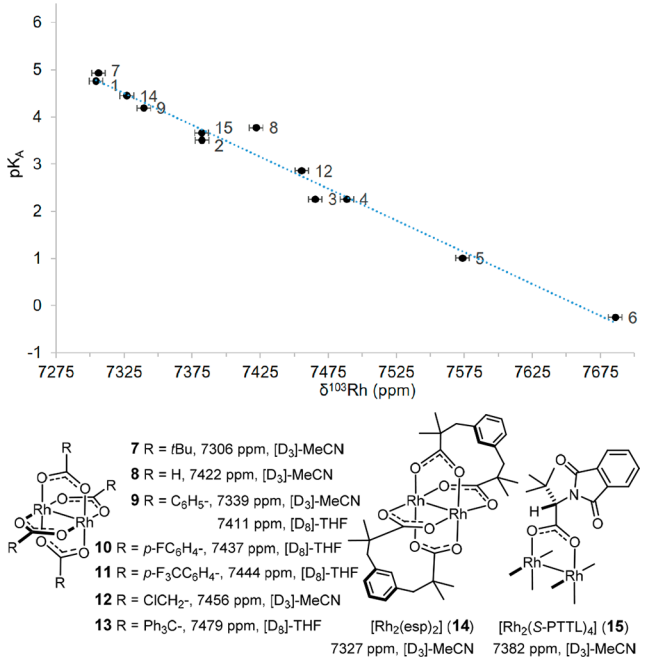

Figure 4. Additional ^{103}Rh chemical shift data (298 K, referenced to $\Xi(^{103}\mathrm{Rh})$ = 3.16%) and correlation with the pK_A of the parent carboxylic acids.

shifts can be correlated with the pK_A values of the parent acids,[47] which capture their donor strengths. Yet, all data fall into a fairly "narrow" shift window (especially if one disregards the highly fluorinated derivatives **5** and **6**), which indicates that the electronic character of the dirhodium core barely changes. One can hence safely conclude that peripheral modifications of the paddlewheels, as practiced in asymmetric catalysis, will hardly change the electronic nature of the catalyst and the derived selectivity-determining transition state.

The "modest" shift range of the tetracarboxylate complexes is best appreciated by a comparison with dirhodium paddlewheels comprised of one or more N-based ligands (Scheme 3A).[48] The arguably most instructive example is the heteroleptic complex **16**, since the incorporation of a single −NH group sets the signals of the now chemically different Rh

Scheme 3. ^{103}Rh Chemical Shifts of Carboxamidate-Based and Heterobimetallic Complexes

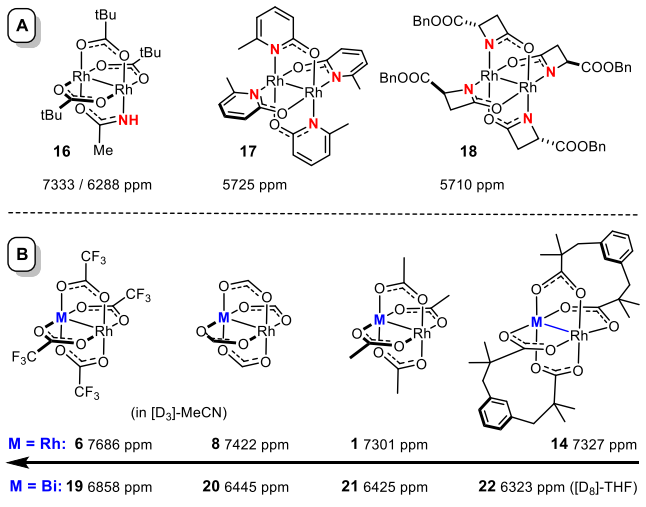

sites >1000 ppm apart. This finding has implications for catalysis, as a chiral relative of **16** was recently shown to be uniquely effective in asymmetric cyclopropanation reactions of α-stannyl(silyl) α-diazoesters.[49] Indirect evidence suggested that these reactions proceed at the rhodium face carrying the protic −NH group, which according to the shift data is the (much) less electrophilic site; this conclusion clearly mandates further scrutiny. In any case, ^{103}Rh NMR makes it unambiguously clear that carboxylate- and carboxamidate-based paddlewheel complexes are very distinct types of catalysts in electronic terms.[48]

A similar conclusion must be drawn for heterobimetallic [BiRh]-paddlewheel catalysts.[50−53] They are known to afford much more electrophilic carbene complexes and perform particularly well in asymmetric cyclopropanation reactions.[53−56] That the 4d orbitals of the Rh(+2) center will sense the incorporation of the sixth-row main group element bismuth as a "metalloligand" is obvious; shift differences of again up to 1000 ppm showcase the magnitude of the effect (Scheme 3B).[46]

Case studies are known in the literature in which the shift of rhodium complexes (or derived reactive intermediates) could be correlated with catalytic performance, but the number is conspicuously small.[2,57−63] With the technical problems in recording pertinent ^{103}Rh NMR spectra come the challenges in interpreting the data, as many different parameters play roles that often prove difficult to disentangle[1−3] even by computational means.[64−66] Arguably, however, dirhodium tetracarboxylate complexes in general and the comprehensive subset **1**−**6** in particular are ideally suited for this type of analysis. They all are comprised of the same rigid "lantern" core, and changes in the bite angles and the Rh−O distances are small and secondary interactions within the ligand sphere minute. Hence, the incremental shift changes when going from $[Rh_2(OAc)_4]$ (**1**) to $[Rh_2(OTfa)_4]$ (**6**) basically reflect electronic rather than geometric changes. A qualitative comparison was therefore deemed legitimate, and a quantitative analysis of the relevant shielding tensors was facilitated because the principal axes coincide in all cases.

Contingent upon the careful optimization of the geometries, the computed shift values reproduce the experimental values remarkably well (Table 1).[67−71] Differences of no more than 0−36 ppm (on a scale of 12.000 ppm) imply that the chosen level of theory provides an accurate description of complexes

Table 1. Comparison between Computed and Experimental ^{103}Rh Chemical Shifts[a,b]

complex	δ_{exp}	δ_{calc}	q	HOMO	LUMO	ΔE
1	0	0	−0.504	−0.1882	−0.0601	0.1281
2	78	80	−0.492	−0.1953	−0.0709	0.1244
3	161	152	−0.48	−0.2053	−0.0790	0.1263
4	184	169	−0.48	−0.2030	−0.0828	0.1202
5	269	275	−0.467	−0.2133	−0.0906	0.1227
6	382	346	−0.455	−0.2238	−0.0997	0.1241

[a]The shift of compound **1** (δ_{Rh} = 7301 ppm) served as a reference. [b]Geometry optimization is as follows: B3LYP-D3/def2-TZVPP, CPCM (MeCN)). NMR shifts are as follows: GIAO-ZORA-TPSSh/decontracted SARC-ZORA-TZVPP (Rh), def2-TZVPP (other nuclei), CPCM(MeCN); q is the Löwdin atomic charges at Rh; and ΔE is the HOMO − LUMO gap.

https://doi.org/10.1021/jacs.1c06414
J. Am. Chem. Soc. 2021, 143, 12473−12479

of this type. Based on this solid foundation, a more detailed analysis is possible and warranted.

As shown above, increasing the fluorination of the acetate ligands causes deshielding. The reduced donor ability of the fluorinated ligands renders the complexes increasingly electrophilic; indeed, the computed ^{103}Rh chemical shifts can be correlated with the partial charge at Rh (Table 1). Although this picture is intuitive and may provide *rough* guidance for the practitioner, it is—at least—oversimplified. Note that the computed energy of the LUMO decreases when going from **1** to **6**, as expected, but the energy of the HOMO drops to a similar extent such that ΔE remains essentially constant. The HOMO − LUMO gap alone does obviously not explain the observed results.

NMR shifts are neither primarily determined by the charge at the metal nor solely by the frontier orbitals. Rather, a chemical shift is an anisotropic property (even though solution NMR spectroscopy provides only the isotropic shift ($\delta_{iso} = (\delta_{11} + \delta_{22} + \delta_{33})/3$). Computational methods allow the individual components of the shielding tensor σ ($\delta_{ii} = \sigma_{iso,ref} - \sigma_{ii}$) to be deconvoluted; it is the paramagnetic term ($\sigma = \sigma_{dia} + \sigma_{para}$) that largely determines the shift of a transition metal nucleus.[72]

The paramagnetic contributions arise from magnetically induced admixture of electronically excited states into the electronic ground state by the angular momentum operator ($\hat{L}_i$) as described by the Ramsey equation (see the Supporting Information).[73] Deshielding in the direction $\sigma_{ii,para}$ depends on which orbitals ϕ_{occ} and ϕ_{vir} can be coupled via $\hat{L}_i$ and on their relative energies: the smaller the energy gap, the larger the effect.

For complexes **1**−**6**, the dominant contributions to $\sigma_{ii,para}$ stem from interactions of the key frontier orbitals (Figure 5).

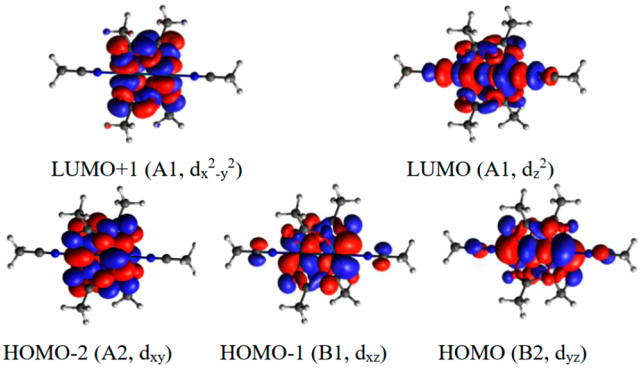

Figure 5. Relevant molecular orbitals of **1** (the associated irreducible representation in the C_{2v} molecular point group and the Rh d orbital associated with each MO are shown in brackets).

As expected, all MOs are delocalized over both Rh centers. Due to symmetry, the only nonzero contributions to the $\sigma_{zz,para}$ component stem from the coupling of the virtual orbitals with the HOMO − 2 (d_{xy}), which is delocalized over the ligands on both axes. As a consequence, $\sigma_{zz,para}$ is always affected by fluorination, irrespective of the position of the halogen atoms. The largest contributions to $\sigma_{yy,para}$ originate from the coupling of the virtual orbitals with the HOMO − 1 (d_{xz}) orbital, which is mostly delocalized over the ligands on the *x*-axis. Similarly, the largest contributions to $\sigma_{xx,para}$ originate from the coupling of the virtual orbitals with the HOMO (d_{yz}) orbital, which is mostly delocalized over the ligands on the *y*-axis. Hence, $\sigma_{yy,para}$ and $\sigma_{xx,para}$ mainly respond to fluorination on the *perpendicular* *x*- and *y*-axes, respectively. Figure 6 illustrates this effect, as only $\delta_{zz,para}$ shows a near linear correlation with the total

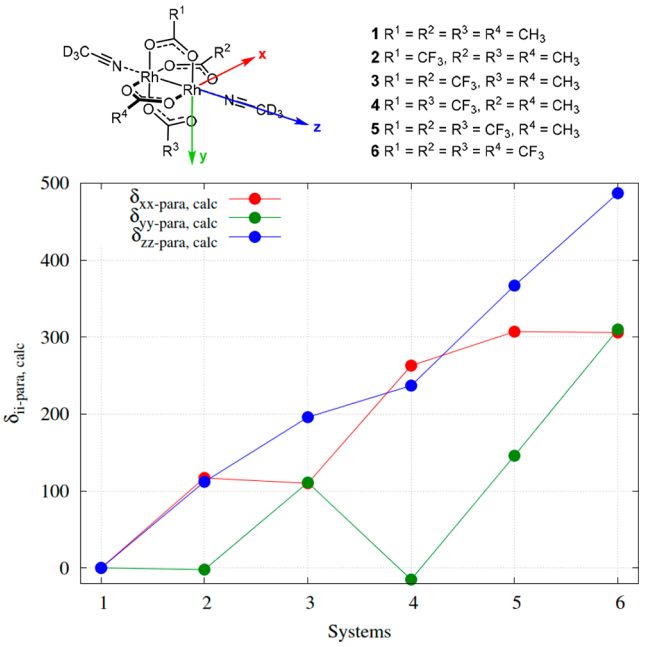

Figure 6. (Top) Principal axis of the shielding tensor of Rh. (Bottom) The paramagnetic contribution to each principal component of the shielding tensor for complexes **1**−**6**.

chemical shift and increases with the increasing fluorination; in contrast, $\delta_{yy,para}$ is roughly constant for **1**, **2**, and **4**, all of which are nonfluorinated along the *x*-axis, while $\delta_{xx,para}$ is basically constant for complexes **4**, **5**, and **6**, which are fully fluorinated along the *y*-axis. Analysis of a given shielding tensor hence provides information about the donor strength of the ligand at the perpendicular position of the lantern core.

The subtleties within this series notwithstanding, one will hardly go wrong in assuming that the ≈880 ppm shift difference between $[Rh_2(OAc)_4]$ (**1**) and $[BiRh(OAc)_4]$ (**21**) bears witness of a drastically different electronic character (Scheme 3). An accurate assessment requires the same kind of analysis as outlined above for the (partly) fluorinated complexes; qualitatively, however, the massive upfield shift suggests that the Rh center, which is the catalytically relevant site of **21**,[53,56] is (much) less electrophilic. The situation in the heteroleptic species **16** is similarly intuitive; because of its relevance, however, a more detailed profiling is subject to ongoing studies. Likewise, we are using the H(C)Rh triple resonance experiment for investigations into other previously uncompliant rhodium complexes, including (highly) reactive intermediates.[74−77] Pertinent results will be reported in due course.

■ ASSOCIATED CONTENT

Supporting Information

The Supporting Information is available free of charge at https://pubs.acs.org/doi/10.1021/jacs.1c06414.

Experimental Section containing supporting NMR data and computational data (PDF)

https://doi.org/10.1021/jacs.1c06414
J. Am. Chem. Soc. 2021, 143, 12473−12479

AUTHOR INFORMATION

Corresponding Authors

Markus Leutzsch − *Max-Planck-Institut für Kohlenforschung, 45470 Mülheim, Germany;* orcid.org/0000-0001-8171-9399; Email: leutzsch@kofo.mpg.de

Alois Fürstner − *Max-Planck-Institut für Kohlenforschung, 45470 Mülheim, Germany;* orcid.org/0000-0003-0098-3417; Email: fuerstner@kofo.mpg.de

Authors

Fabio P. Caló − *Max-Planck-Institut für Kohlenforschung, 45470 Mülheim, Germany*

Giovanni Bistoni − *Max-Planck-Institut für Kohlenforschung, 45470 Mülheim, Germany;* orcid.org/0000-0003-4849-1323

Alexander A. Auer − *Max-Planck-Institut für Kohlenforschung, 45470 Mülheim, Germany;* orcid.org/0000-0001-6012-3027

Complete contact information is available at: https://pubs.acs.org/10.1021/jacs.1c06414

Funding

Open access funded by Max Planck Society.

Notes

The authors declare no competing financial interest.

ACKNOWLEDGMENTS

Generous financial support by the Fonds der Chemischen Industrie (Kekulé stipend to F.P.C.) and the Max-Planck-Society is gratefully acknowledged. We thank Dr. C. Farès for valuable discussions and all analytical departments of our Institute for excellent support.

REFERENCES

(1) Carlton, L., Rhodium-103 NMR. In *Annual Reports on NMR Spectroscopy*, Vol. *63*; Webb, G. A., Ed. Academic Press: London, U.K., 2008; pp 49−178.

(2) Ernsting, J. M.; Gaemers, S.; Elsevier, C. J. ^{103}Rh NMR spectroscopy and its application to rhodium chemistry. *Magn. Reson. Chem.* **2004**, *42* (9), 721−736.

(3) Mann, B. E. The Cinderella Nuclei. *Annu. Rep. NMR Spectrosc.* **1991**, *23*, 141−207.

(4) Benn, R.; Rufińska, A. High-Resolution Metal NMR Spectroscopy of Organometallic Compounds. *Angew. Chem., Int. Ed. Engl.* **1986**, *25* (10), 861−881.

(5) Especially in case of rather small and symmetrical complexes, see: Benn, R.; Brenneke, H.; Reinhardt, R.-D. ^{103}Rh NMR at 9.4 T - Improved Signal Detection Due to Shortened Relaxation Times and Selective Polarization Transfer. *Z. Naturforsch., B: J. Chem. Sci.* **1985**, *40*, 1763−1765.

(6) For selected examples of direct detection, see: (a) Gill, D. S.; Gansow, O. A.; Bennis, F. J.; Ott, K. C. The Direct Observation of ^{103}Rh NMR. *J. Magn. Reson.* **1979**, *35*, 459−461.

(7) Grüninger, K.-D.; Schwenk, A.; Mann, B. E. Direct observation of ^{103}Rh NMR and relaxation investigations by steady-state techniques. *J. Magn. Reson.* **1980**, *41* (2), 354−357.

(8) Maurer, E.; Rieker, S.; Schollbach, M.; Schwenk, A.; Egolf, T.; von Philipsborn, W. Direct Observation of ^{103}Rh-Chemical Shifts in Mono- and Dinuclear Olefin Complexes. *Helv. Chim. Acta* **1982**, *65* (1), 26−45.

(9) Doyle, M. P.; McKervey, M. A.; Ye, T. *Modern Catalytic Methods for Organic Synthesis with Diazo Compounds: From Cyclopropanes to Ylides*; Wiley: Hoboken, NJ, 1998.

(10) Ford, A.; Miel, H.; Ring, A.; Slattery, C. N.; Maguire, A. R.; McKervey, M. A. Modern Organic Synthesis with α-Diazocarbonyl Compounds. *Chem. Rev.* **2015**, *115* (18), 9981−10080.

(11) Doyle, M. P.; Duffy, R.; Ratnikov, M.; Zhou, L. Catalytic Carbene Insertion into C-H Bonds. *Chem. Rev.* **2010**, *110*, 704−724.

(12) Davies, H. M. L.; Manning, J. R. Catalytic C-H functionalization by metal carbenoid and nitrenoid insertion. *Nature* **2008**, *451* (7177), 417−424.

(13) Zhu, S. F.; Zhou, Q. L. Transition-Metal-Catalyzed Enantioselective Heteroatom-Hydrogen Bond Insertion Reactions. *Acc. Chem. Res.* **2012**, *45*, 1365.

(14) DeAngelis, A.; Panish, R.; Fox, J. M. Rh-Catalyzed Intermolecular Reactions of α-Alkyl-α-Diazo Carbonyl Compounds with Selectivity over β-Hydride Migration. *Acc. Chem. Res.* **2016**, *49*, 115.

(15) Lebel, H.; Marcoux, J. F.; Molinaro, C.; Charette, A. B. Stereoselective Cyclopropanation Reactions. *Chem. Rev.* **2003**, *103*, 977.

(16) Hrdina, R. Dirhodium(II,II) Paddlewheel Complexes. *Eur. J. Inorg. Chem.* **2021**, *2021*, 501−528.

(17) For applications beyond catalysis, see refs 16, 18−21 and the following, as well as literature cited therein: Chifotides, H. T.; Dunbar, K. R. Interactions of Metal-Metal-Bonded Antitumor Active Complexes with DNA Fragments and DNA. *Acc. Chem. Res.* **2005**, *38* (2), 146−156.

(18) Ohata, J.; Ball, Z. T. Rhodium at the chemistry-biology interface. *Dalton Trans.* **2018**, *47* (42), 14855−14860.

(19) Dunham, S. U.; Remaley, T. S.; Moore, B. S.; Evans, D. L.; Dunham, S. U. Isolation, Characterization, and DNA Binding Kinetics of Three Dirhodium(II,II) Carboxyamidate Complexes: $Rh_2(\mu\text{-}L)(HNOCCF_3)_3$ where L= $[OOCCH_3]$-, $[OOCCF_3]$-, or $[HNOCCF_3]$-. *Inorg. Chem.* **2011**, *50* (8), 3458−3463.

(20) Felder, P. S.; Keller, S.; Gasser, G. Polymetallic Complexes for Applications as Photosensitisers in Anticancer Photodynamic Therapy. *Advanced Therapeutics* **2020**, *3* (1), 1900139.

(21) Tanaka, S.; Masaoka, S.; Yamauchi, K.; Annaka, M.; Sakai, K. Photochemical and thermal hydrogen production from water catalyzed by carboxylate-bridged dirhodium(ii) complexes. *Dalton Trans.* **2010**, *39* (46), 11218−11226.

(22) What is known are the ^{103}Rh NMR shifts of a few (phosphine, phosphite, nucleobase) adducts and $[Rh_2(mhp)_4]$ (**17**, mhp = 6-methyl-2-hydroxypyridine) (see refs 23−27); such complexes have no immediate relevance for catalysis. Moreover, $[Rh_2(OTfa)_4]$ does not even form stable adducts with phosphites, but instead undergoes redox reactions, see: Boyar, E. B.; Robinson, S. D. Complexes of the Platinum Metals. Part 26. Multinuclear Nuclear Magnetic Resonance Studies on Rhodium(II) Carboxylate Adducts. *J. Chem. Soc., Dalton Trans.* **1985**, 629−633.

(23) Boyar, E. B.; Robinson, S. D. Multinuclear NMR studies on rhodium(II) acetate-trimethylphosphite adducts. *Inorg. Chim. Acta* **1982**, *64*, L193−L194.

(24) Magiera, D.; Baumann, W.; Podkorytov, I. S.; Omelanczuk, J.; Duddeck, H. Stable $Rh_2(MTPA)_4$ Phosphane Adducts - The First Example of P-Chirality Recognition by ^{103}Rh NMR Spectroscopy. *Eur. J. Inorg. Chem.* **2002**, *2002* (12), 3253−3257.

(25) Heaton, B. T.; Iggo, J. A.; Podkorytov, I. S.; Tunik, S. P. Application of HMQC spectroscopy to the observation of the metal resonance in polymetallic compounds: the effect of multiple-metal spin transitions. *Magn. Reson. Chem.* **2004**, *42* (9), 769−775.

(26) Garner, C. D.; Berry, M.; Mann, B. E. Rhodium-103 NMR spectrum of $[(Rh_2(mhp)_4)_2]$: the first measurement of ^1J(rhodium-103, rhodium-103) for a $[Rh_2]^{4+}$ core. *Inorg. Chem.* **1984**, *23* (11), 1500−1501.

(27) Catalan, K. V.; Hess, J. S.; Maloney, M. M.; Mindiola, D. J.; Ward, D. L.; Dunbar, K. R. Reactions of DNA Purines with Dirhodium Formamidinate Compounds That Display Antitumor Behavior. *Inorg. Chem.* **1999**, *38* (17), 3904−3913.

(28) For recent use of transition metal NMR spectroscopy for catalysis research from this group, see refs 29 and 30 and the

following: Hillenbrand, J.; Leutzsch, M.; Fürstner, A. Molybdenum Alkylidyne Complexes with Tripodal Silanolate Ligands. The Next Generation of Alkyne Metathesis Catalysts. *Angew. Chem., Int. Ed.* **2019**, *58*, 15690−15696.
(29) Hillenbrand, J.; Leutzsch, M.; Yiannakas, E.; Gordon, C. P.; Wille, C.; Nöthling, N.; Copéret, C.; Fürstner, A. Canopy Catalysts" for Alkyne Metathesis: Molybdenum Alkylidyne Complexes with a Tripodal Ligand Framework. *J. Am. Chem. Soc.* **2020**, *142* (25), 11279−11294.
(30) Hillenbrand, J.; Leutzsch, M.; Gordon, C. P.; Copéret, C.; Fürstner, A. ^{183}W NMR Spectroscopy Guides the Search for Tungsten Alkylidyne Catalysts for Alkyne Metathesis. *Angew. Chem., Int. Ed.* **2020**, *59*, 21758−21768.
(31) Gudat, D. Indirect detection of ^{31}P,X connectivities with proton sensitivity: application of two-dimensional ^{31}P-relayed ^{1}H,X correlation spectroscopy. *Magn. Reson. Chem.* **2003**, *41* (4), 253−259.
(32) Mobley, T. A.; Tennyson, E. G.; Hisao, G. S. Indirect detection of the ^{183}W and ^{57}Fe nuclei using ^{119}Sn-relayed ^{1}H,X correlation spectroscopy. *Magn. Reson. Chem.* **2010**, *48* (10), 787−792.
(33) For other uses, see refs 34 and 35 and the following: Malon, M.; Takahashi, S.; Koshino, H. A New Method for Determining Positions of Phenolic Hydroxyl Groups Through Silylation and Application of H(Si)C Triple-resonance NMR Experiments. *Tetrahedron Lett.* **2007**, *48*, 7586−7590.
(34) Maloň, M.; Imakubo, T.; Koshino, H. ^{1}H, ^{13}C and ^{77}Se NMR study of tetraselenafulvalene derivatives supported by novel H(Se)C and H(C)Se triple-resonance experiments at natural abundance. *Magn. Reson. Chem.* **2008**, *46* (2), 150−155.
(35) Weske, S.; Li, Y.; Wiegmann, S.; John, M. H(C)Ag: a triple resonance NMR experiment for ^{109}Ag detection in labile silver-carbene complexes. *Magn. Reson. Chem.* **2015**, *53* (4), 291−294.
(36) As the X-channel pulses of low-γ nuclei such as ^{103}Rh are often difficult to determine and need relatively high powers, the HMQC transfer offers an advantage as it is less sensitive to miscalibrated pulses.
(37) The strong temperature dependence disqualifies [Rh(acac)$_3$] as the "standard" for referencing ^{103}Rh NMR shifts; the consensus is to reference the ^{103}Rh shifts to an absolute frequency related to the resonance frequency of the protons of tetramethylsilane ($\Xi(^{103}\mathrm{Rh})$ = 3.16%), cf. ref 1.
(38) During the acquisition, a selective low-power ^{13}C decoupling on the C═O resonance was used. A higher decoupling power could influence the temperature of the sample and therefore the reproducibility of the ^{103}Rh NMR shifts.
(39) Xiang, B.; Winemiller, M. D.; Briggs, T. F.; Fuller, D. J.; Collum, D. B. Optimizing HMQC for IS$_n$ spin systems. *Magn. Reson. Chem.* **2001**, *39* (3), 137−140.
(40) The recorded shift was identical within the experimental error with the shift determined by conventional ^{13}C, ^{103}Rh-HMBC experiments. Note, however, that an ordinary sample of the complex sufficed for the triple resonance experiment, whereas the HMBC spectra mandated the use of ^{13}C-labeled acetate ligands (at C1 or C2). An analogous control experiment using ^{13}C-labeled acetate was performed with [BiRh(OAc)$_4$].
(41) For this reason, we expect ^{103}Rh chemical shifts to vary by 5 ppm in different experiments, unless the temperature is very carefully controlled.
(42) The binding of an axial ligand involves the Rh−Rh B* orbital; raising the energy of this low-lying unoccupied orbital is expected to affect the shift according to the Ramsey equation (see below). For a general discussion of the three-center or four-electron bonding in dirhodium paddlewheel complexes, see: Berry, J. F. The Role of Three-Center/Four-Electron Bonds in Superelectrophilic Dirhodium Carbene and Nitrene Catalytic Intermediates. *Dalton Trans.* **2012**, *41*, 700−713.
(43) For the higher kinetic stability of this adduct, one expects two distinct Rh resonances; however, only one signal was recorded for reasons that are currently unclear.
(44) To appreciate the effect, the reader is reminded of a previous report that showed that the ^{19}F NMR signal of [Rh$_2$(OTfa)$_4$] hardly changes ($\Delta\delta$ = 0.2 ppm) upon the coordination of a *tert*-amine to the axial site, even though ^{19}F NMR has a shift range of several hundred parts per million and is hence usually deemed highly responsive, see: Jazwinski, J. Studies on Adducts of Rhodium(II) Tetraacetate and Rhodium(II) Tetratrifluoroacetate with some Amines in $CDCl_3$ Solution Using ^{1}H, ^{13}C, and ^{15}N NMR. *J. Mol. Struct.* **2005**, *750*, 7−17.
(45) Lou, Y.; Remarchuk, T. P.; Corey, E. J. Catalysis of Enantioselective [2 + 1]-Cycloaddition Reactions of Ethyl Diazoacetate and Terminal Acetylenes Using Mixed-Ligand Complexes of the Series Rh$_2$(RCO$_2$)$_n$ (L*4-n). Stereochemical Heuristics for Ligand Exchange and Catalyst Synthesis. *J. Am. Chem. Soc.* **2005**, *127* (41), 14223−14230.
(46) Because [Rh$_2$(OTfa)$_4$] and [BiRh(OTfa)$_4$] do not contain a proton, the triple resonance experiment as described herein cannot be applied; the shift of this complex had to be determined by 1D NMR spectroscopy using highly concentrated samples.
(47) In case of the heteroleptic complexes, an "averaged" pK_A was chosen; see the Supporting Information.
(48) Doyle, M. P. Perspective on Dirhodium Carboxamidates as Catalysts. *J. Org. Chem.* **2006**, *71* (25), 9253−9260.
(49) Caló, F.; Fürstner, A. A Heteroleptic Dirhodium Catalyst for Asymmetric Cyclopropanation with α-Stannyl-α-Diazoacetate. 'Stereoretentive' Stille Coupling with Formation of Chiral Quarternary Centers. *Angew. Chem., Int. Ed.* **2020**, *59*, 13900.
(50) Dikarev, E. V.; Li, B.; Zhang, H. Tuning the Properties at Heterobimetallic Core: Mixed-Ligand Bismuth-Rhodium Paddlewheel Carboxylates. *J. Am. Chem. Soc.* **2006**, *128*, 2814.
(51) Filatov, A. S.; Napier, M.; Vreshch, V. D.; Sumner, N. J.; Dikarev, E. V.; Petrukhina, M. A. From Solid State to Solution: Advancing Chemistry of Bi-Bi and Bi-Rh Paddlewheel Carboxylates. *Inorg. Chem.* **2012**, *51*, 566.
(52) Hansen, J.; Li, B.; Dikarev, E.; Autschbach, J.; Davies, H. M. L. Combined Experimental and Computational Studies of Heterobimetallic Bi-Rh Paddlewheel Carboxylates as Catalysts for Metal Carbenoid Transformations. *J. Org. Chem.* **2009**, *74*, 6564.
(53) Collins, L. R.; van Gastel, M.; Neese, F.; Fürstner, A. Enhanced Electrophilicity of Heterobimetallic Bi-Rh Paddlewheel Carbene Complexes: A Combined Experimental, Spectroscopic and Computational Study. *J. Am. Chem. Soc.* **2018**, *140*, 13042.
(54) Collins, L. R.; Auris, S.; Goddard, R.; Fürstner, A. Chiral Heterobimetallic Bismuth-Rhodium Paddlewheel Catalysts: A Conceptually New Approach to Asymmetric Cyclopropanation. *Angew. Chem., Int. Ed.* **2019**, *58*, 3557.
(55) Singha, S.; Buchsteiner, M.; Bistoni, G.; Goddard, R.; Fürstner, A. A New Ligand Design Based on London Dispersion Empowers Chiral Bismuth-Rhodium Paddlewheel Catalysts. *J. Am. Chem. Soc.* **2021**, *143* (15), 5666−5673.
(56) Löffler, L. E.; Buchsteiner, M.; Collins, L. R.; Caló, F. P.; Singha, S.; Fürstner, A. [Rh$_2$(MEPY)$_4$] and [BiRh(MEPY)$_4$]: Convenient Syntheses and Computational Analysis of Strikingly Dissimilar Siblings. *Helv. Chim. Acta* **2021**, *104*, No. e2100042.
(57) von Philipsborn, W. Probing organometallic structure and reactivity by transition metal NMR spectroscopy. *Chem. Soc. Rev.* **1999**, *28* (2), 95−105.
(58) For a timely discussion of how to probe structure−activity relationships by (transition metal) NMR, see: Gordon, C. P.; Lätsch, L.; Copéret, C. Copéret, C. Nuclear Magnetic Resonance: A Spectroscopic Probe to Understand the Electronic Structure and Reactivity of Molecules and Materials. *J. Phys. Chem. Lett.* **2021**, *12*, 2072−2085.
(59) For some leading references, see refs 60−66 and the following: Bender, B. R.; Koller, M.; Nanz, D.; von Philipsborn, W. ^{103}Rh Shielding and the Stereoselectivity of H2 Addition to Diasteromeric Olefin Complexes. *J. Am. Chem. Soc.* **1993**, *115*, 5889−5890.
(60) Koller, M.; von Philipsborn, W. Transition metal NMR spectroscopy. 19. Correlation of rhodium-103 NMR shielding and

https://doi.org/10.1021/jacs.1c06414
J. Am. Chem. Soc. 2021, 143, 12473−12479

rate constants of carbonyl displacement reactions in (o^5-C_5H_4X)Rh-$(CO)_2$ complexes. *Organometallics* **1992**, *11* (1), 467−469.
(61) Aakermark, B.; Blomberg, M. R. A.; Glaser, J.; Oehrstroem, L.; Wahlberg, S.; Waernmark, K.; Zetterberg, K. The Metal-Alkene Bond in Rh(I)((-diketonato)(alkene)$_2$ Complexes. Correlation of ^{103}Rh-NMR Shifts with Stability Constants, Alkene Excitation Energies, and d-d Absorption Bands. An Experimental and Theoretical Study. *J. Am. Chem. Soc.* **1994**, *116* (8), 3405−3413.
(62) Fornika, R.; Görls, H.; Seemann, B.; Leitner, W. Complexes [(P_2)Rh(hfacac)] (P_2 = bidentate chelating phosphane, hfacac = hexafluoroacetylacetonate) as catalysts for CO_2 hydrogenation: correlations between solid state structures, ^{103}Rh NMR shifts and catalytic activities. *J. Chem. Soc., Chem. Commun.* **1995**, No. 14, 1479−1481.
(63) Leitner, W.; Bühl, M.; Fornika, R.; Six, C.; Baumann, W.; Dinjus, E.; Kessler, M.; Krüger, C.; Rufińska, A. ^{103}Rh Chemical Shifts in Complexes Bearing Chelating Bidentate Phosphine Ligands. *Organometallics* **1999**, *18* (7), 1196−1206.
(64) Bühl, M. Substituent Effects on ^{103}Rh NMR Chemical Shifts and Reactivities. A Density Functional Study. *Organometallics* **1997**, *16* (2), 261−267.
(65) Mirzaeva, I. V.; Mainichev, D. A.; Kozlova, S. G. A Localized Molecular Orbital Study of the Halogen Substitution Effect on ^{103}Rh NMR Shielding in [Cp^*RhX_2]$_2$, Where X = Cl, Br, or I. *J. Phys. Chem. A* **2016**, *120* (11), 1944−1949.
(66) Orian, L.; Bisello, A.; Santi, S.; Ceccon, A.; Saielli, G. ^{103}Rh NMR Chemical Shifts in Organometallic Complexes: A Combined Experimental and Density Functional Study. *Chem. - Eur. J.* **2004**, *10* (16), 4029−4040.
(67) Bouten, R.; Baerends, E. J.; van Lenthe, E.; Visscher, L.; Schreckenbach, G.; Ziegler, T. Relativistic Effects for NMR Shielding Constants in Transition Metal Oxides Using the Zeroth-Order Regular Approximation. *J. Phys. Chem. A* **2000**, *104* (23), 5600−5611.
(68) Stoychev, G. L.; Auer, A. A.; Izsák, R.; Neese, F. Self-Consistent Field Calculation of Nuclear Magnetic Resonance Chemical Shielding Constants Using Gauge-Including Atomic Orbitals and Approximate Two-Electron Integrals. *J. Chem. Theory Comput.* **2018**, *14* (2), 619−637.
(69) Pantazis, D. A.; Chen, X.-Y.; Landis, C. R.; Neese, F. All-Electron Scalar Relativistic Basis Sets for Third-Row Transition Metal Atoms. *J. Chem. Theory Comput.* **2008**, *4* (6), 908−919.
(70) Stoychev, G. L.; Auer, A. A.; Neese, F. Automatic Generation of Auxiliary Basis Sets. *J. Chem. Theory Comput.* **2017**, *13* (2), 554−562.
(71) van Lenthe, E.; Snijders, J. G.; Baerends, E. J. The zero-order regular approximation for relativistic effects: The effect of spin-orbit coupling in closed shell molecules. *J. Chem. Phys.* **1996**, *105* (15), 6505−6516.
(72) For the complexes of this series, σ_{dia} is almost constant.
(73) Ramsey, N. F. Magnetic Shielding of Nuclei in Molecules. *Phys. Rev.* **1950**, *78*, 699−703.
(74) Werlé, C.; Goddard, R.; Fürstner, A. The First Crystal Structure of a Reactive Dirhodium Carbene Complex and a Verstatile New Method for the Preparation of Gold Carbenes by Rhodium-to-Gold Transmetalation. *Angew. Chem., Int. Ed.* **2015**, *54*, 15452−15456.
(75) Werlé, C.; Goddard, R.; Philipps, P.; Farès, C.; Fürstner, A. Structures of Reactive Donor/Acceptor and Donor/Donor Rhodium Carbenes in the Solid State and Their Implication for Catalysis. *J. Am. Chem. Soc.* **2016**, *138*, 3797−3805.
(76) Werlé, C.; Goddard, R.; Philipps, P.; Farès, C.; Fürstner, A. Stabilization of a Chiral Dirhodium Carbene by Encapsulation and a Discussion of the Stereochemical Implications. *Angew. Chem., Int. Ed.* **2016**, *55*, 10760−10765.
(77) Tindall, D. J.; Werlé, C.; Goddard, R.; Philipps, P.; Farès, C.; Fürstner, A. Structure and Reactivity of Half-Sandwich Rh(+3) and Ir(+3) Carbene Complexes. Catalytic Metathesis of Azobenzene Derivatives. *J. Am. Chem. Soc.* **2018**, *140*, 1884−1893.

https://doi.org/10.1021/jacs.1c06414
J. Am. Chem. Soc. 2021, 143, 12473−12479